

Diabolical Points in Molecular Magnets with a Four-Fold Easy Axis

Chang-Soo Park* and Anupam Garg**

Department of Physics and Astronomy, Northwestern University, Evanston, Illinois 60208

(November 13, 2018)

Abstract

We study the points of degeneracy (diabolical points) in magnetic molecules such as Mn_{12} -acetate that have an easy axis of four-fold symmetry. This is done for general magnetic field that need not be oriented along a high-symmetry direction. We develop a perturbative technique that gives the diabolical points as the roots of a small number of polynomials in the transverse component of the magnetic field and the fourth order basal plane anisotropy. In terms of these roots we obtain approximate analytic formulas that apply to any system with total spin $S \leq 10$. The analytic results are found to compare reasonably well with exact numerical diagonalization for the case of Mn_{12} . In addition, the perturbation theory shows that the diabolical points may be indexed by the magnetic quantum numbers of the levels involved, even at large transverse fields. Certain points of degeneracy are found to be mergers (or near mergers) of two or three diabolical points because of the symmetry of the problem.

75.10Dg, 03.65.Db, 03.65.Sq, 75.45.+j, 75.50.Xx

I. INTRODUCTION

The magnetic molecules Mn_{12} [short for Mn_{12} -acetate, or $[\text{Mn}_{12}(\text{CH}_3\text{COO})_{16}(\text{H}_2\text{O})_4\text{O}_{12}] \cdot 2\text{CH}_3\text{COOH} \cdot 4\text{H}_2\text{O}$] and Fe_8 [short for $\text{Fe}_8\text{O}_2(\text{OH})_{12}(\text{tacn})_6^{8+}$] are among a few dozen that are currently being studied as extreme cases of superparamagnets [1]. Both Mn_{12} and Fe_8 have spin 10, and both of them display hysteresis at the molecular level [2–5], as do some of the others. In addition, however, Fe_8 shows an effect that has not yet been seen in any of the other molecules: oscillation of the Landau-Zener-Stückelberg transition rate between low lying levels as a function of the applied static magnetic field [6]. This oscillation is due to an oscillatory quenching of the underlying tunneling matrix element connecting the levels in question, and is an unambiguous signature of quantum tunneling. The occurrence and observability of tunneling in a spin of such a large magnitude is of much interest in itself, and the tunneling frequency, of the order of 100 Hz, is perhaps the lowest ever inferred or measured in any physical system. Further, the quenching effect can be regarded as due to the interference of different Feynman tunneling paths for the spin [7], and this is how it was first discovered [8]. While massive particle tunneling in two or more spatial dimensions can also show such interference [9], the effect arises more directly in the spin problem since the kinetic term in the action has the mathematical structure of a Berry phase. This adds to the interest in the problem. Reciprocally, the experimental observations have motivated more careful investigations of spin-coherent-state path integrals which are more delicate than their massive particle counterparts [10].

The above interference effect has also been sought in Mn_{12} , but has not yet been seen. While the spin Hamiltonian for Fe_8 has biaxial symmetry, Mn_{12} is tetragonal, hence the systematics of the effect are different, and it is interesting to calculate them. More specifically, with an external magnetic field \mathbf{H} , Mn_{12} is described by an anisotropy Hamiltonian [11]

$$\mathcal{H} = -AS_z^2 - BS_z^4 + C(S_+^4 + S_-^4) - g\mu_B \mathbf{S} \cdot \mathbf{H}, \quad (1.1)$$

where $S = 10$, $g \approx 2$, and $A \gg B \gg C > 0$. (The experimental values for A , B , and C are 0.556, 1.1×10^{-3} , and 3×10^{-5} K, respectively, so that $\lambda_1 = B/A = 1.98 \times 10^{-3}$, $\lambda_2 = C/A = 5.4 \times 10^{-5}$, and $H_c = A/g\mu_B = 0.414$ T.) The easy axis is now z with four fold symmetry, the hard axes are $\pm x$ and $\pm y$, and the medium axes are the lines $y = \pm x$ in the xy -plane. For values of $|\mathbf{H}|$ that are not too large, the spin coherent state [12] expectation value $\langle \hat{\mathbf{n}} | \mathcal{H} | \hat{\mathbf{n}} \rangle$, which may be regarded as a classical energy $E(\theta, \phi)$, may have two or more local minima, between which the spin can then tunnel. The issue is to calculate the tunnel splitting Δ , and especially the field values where this splitting is quenched, i.e., $\Delta = 0$. Since there may be other molecules with this symmetry, it is desirable to do this analytically, for all values of (or at least a wide range of) λ_1 and λ_2 .

For the discussion that follows, it is useful to review some basic facts pertaining to degeneracy in quantum mechanics in the absence of symmetry. A point of degeneracy, or equivalently, a point where the splitting between two levels vanishes, is *diabolical* in the terminology of Berry and Wilkinson [13], or a *conical intersection* in older terminology [14]. As a rule, eigenvalues of a finite Hamiltonian are all simple, and for a general Hamiltonian, represented by a complex Hermitean matrix, we must be able to adjust at least three parameters in order to produce a degeneracy. A simple approximate argument is as follows [15]. Let two states m and m' be approximately degenerate, and let the secular matrix between them be written as

$$\begin{pmatrix} E_m & V_{mm'} \\ V_{m'm} & E_{m'} \end{pmatrix}, \quad (1.2)$$

with $V_{m'm} = V_{mm'}^*$. The states will be truly degenerate only if the following two conditions are met:

$$B_{mm'} \equiv E_m - E_{m'} = 0, \quad (1.3)$$

$$V_{mm'} = 0. \quad (1.4)$$

It is convenient to refer to these as the no-bias and the no-mixing conditions, respectively [16]. Since $V_{mm'}$ is in general complex, we have three real conditions, requiring three or more variable parameters for their satisfaction.

Precisely three parameters are available to us in Eq. (1.1) in the three components of \mathbf{H} . If the Hamiltonian matrix is real symmetric, the number of adjustable parameters required is lowered to two. In the present problem, this situation is realized when $H_y = 0$, and so, as in the Fe_8 case, we expect to find the degeneracies in the H_x - H_z plane. Unless explicitly stated, we will henceforth take $H_y = 0$, so that $V_{mm'} = V_{m'm}$.

Ignoring an additive constant, the energy surface in the vicinity of the degeneracy is given by

$$E = \pm(B_{mm'}^2 + V_{mm'}^2)^{1/2} \quad (1.5)$$

which has the form of a double cone or a *diabolo* in H_x - H_z space, which explains the term diabolical for these points.

In a previous paper [17], we have studied the Mn_{12} problem for $\mathbf{H} \parallel \hat{\mathbf{x}}$. In this case, $E(\theta, \phi)$ is reflection symmetric in the equatorial plane, and for small enough H , has two degenerate minima, one in each hemisphere with $S_z > 0$ and $S_z < 0$. The problem is analogous to the tunneling of a massive particle in a symmetric double well. The approach used is a discrete phase integral (DPI) or Wentzel-Kramers-Brillouin (WKB) method, and it provides a good quantitative approximation for the tunnel splitting, Δ , as well as the diabolical fields where the splitting vanishes.

In this paper, we extend our studies to the case where the field has a nonzero z component. The problem is now like a massive particle in an asymmetric double well. Our initial intent was to approach this case also using the DPI method, as it has been applied successfully to the Fe_8 problem. Indeed, the calculation reduces to no more than the evaluation of a handful of action integrals, and based on prior experience with Fe_8 and other tunneling Hamiltonians, we are confident that it will be quantitatively accurate for Mn_{12} too. Unlike the Fe_8 case, however, where the integrals can be found analytically, this turns out to be not so for Mn_{12} , and so, even though the calculation is not as atomistic as a brute force diagonalization of the 21×21 Hamiltonian matrix, it still does not yield final answers in an analytic form. To our pleasant surprise, however, we have found that a perturbative approach in the spirit of Ref. [18] not only yields quite good approximations for the locations of the diabolical points, it also reveals a pattern in the points which would be hard to discern from a numerical diagonalization by itself. Most importantly, it provides a scheme for indexing these points. It is the purpose of this paper to report this work.

The analysis is contained in Sec. II. We first develop the perturbation theory with $B = 0$ (Sec. IIA). This yields the diabolical points as the roots of polynomials in H_x and

C. For a given spin S , we have $2S$ polynomials. One of the unexpected bonuses is that a polynomial which applies to a given value of S also applies to any other value of S . We find all these polynomials for $S \leq 10$. In subsection II B, we incorporate the effects of the B term approximately, and compare our analytic results with those from explicit numerical diagonalization of the Hamiltonian with the parameters for Mn_{12} (see Table III). Our results are accurate to about 10% for Mn_{12} , and we believe that they will also be useful for other systems with four-fold anisotropy. This is especially true for the low lying energy levels. In fact, for the higher pairs of levels, the diabolical points can be significantly moved or even eliminated altogether by still higher anisotropy terms in the Hamiltonian. In subsection II C we discuss some qualitative aspects of the degeneracies on the H_z axis, and show that some of them behave as the merger of two or three diabolical points. A short summary (Sec. III) concludes the paper.

II. PERTURBATIVE CALCULATION

Let us first consider the problem when $H_x = 0$, i.e., $\mathbf{H} \parallel \hat{\mathbf{z}}$. The S_{\pm}^4 terms couple states with m differing by 4, and thus divide the Hamiltonian into four disjoint subspaces. Levels belonging to different subspaces can cross at fields which can be approximately obtained by neglecting the S_{\pm}^4 terms. The crossing conditions are $E_m = E_{m'}$, where $E_m = -Am^2 - Bm^4 - g\mu_B H_z m$. Improved formulas can be obtained by finding corrections to E_m perturbatively in C . These intersections are easy to understand because a symmetry of the Hamiltonian (invariance under a rotation by 90° about $\hat{\mathbf{z}}$) is easily recognized.

If H_x and H_z are both non-zero, there is no obvious symmetry. If H_x and C are both small, however, we may continue to label the states by the m quantum numbers, and calculate the energies perturbatively in these two parameters. In terms of the secular matrix (1.2), the energies E_m , $E_{m'}$, and the bias $B_{mm'}$ are determined by the terms in S_z in Eq. (1.1), and the mixing $V_{mm'}$ by the terms involving C and H_x . The energies are trivial to find, so the problem is to find $V_{mm'}$.

It is convenient to divide the Hamiltonian by A and to work with scaled quantities

$$\lambda_1 = B/A, \quad \lambda_2 = C/A, \quad h_{x,z} = H_{x,z}/SH_c, \quad (2.1)$$

with

$$H_c \equiv A/g\mu_B. \quad (2.2)$$

A. Simplified model: $B = 0$.

To keep the problem tractable, let us set $B = 0$ at this stage. Then, to zeroth order in both C and H_x , $E_m = -Am^2 - g\mu_B H_z m$. Hence, levels m and m' are degenerate when

$$h_z = -\frac{m + m'}{S}. \quad (2.3)$$

It remains to find the off-diagonal element $V_{mm'}$. As we shall see, the choice $B = 0$ simplifies the calculation greatly, for E_m is then quadratic in m , and energy level differences are linear in m , and given by a fixed set of numbers whenever Eq. (2.3) holds.

To illustrate the calculation of $V_{mm'}$, we consider the case $S = 5$. Suppose $h_z = 1/5$, so that $m = -5$ and $m' = 4$ are degenerate (see Fig. 1). We will find $V_{4,-5}$ to leading non-zero order in h_x and C as a double series in these variables. It is clear that a transition from m to m' can be made in three ways:

- (1) act with $h_x S_+$ in 9th order.
- (2) act with $h_x S_+$ in 5th order and CS_+^4 in 1st order.
- (3) act with $h_x S_+$ in 1st order and CS_+^4 in 2nd order.

We denote the corresponding contributions to V by $V^{(1)}$, $V^{(2)}$, and $V^{(3)}$. Each of these involves a product of matrix elements and a product of energy denominators. For $V^{(1)}$, the former is

$$\frac{1}{2^9} \langle 5, 4 | S_+^9 | 5, -5 \rangle (-h_x S)^9 = 709\sqrt{10}(-h_x S)^9 \equiv W(-h_x S)^9. \quad (2.4)$$

In fact the number W will be common (up to some power of 2) to all three $V^{(i)}$. The energy denominators can be read off Fig. 1, and for $V^{(1)}$, these are

$$(-1)^8 (8 \times 14 \times 18 \times 20)^2 \equiv (-1)^8 K^2. \quad (2.5)$$

The factor $(-1)^8$ appears here because all intermediate states are higher in energy than E_{-5} and E_4 , and we have introduced the number K because many of the energy denominator products for $V^{(2)}$ and $V^{(3)}$ contain the same factors. Putting together Eqs. (2.4) and (2.5),

$$V^{(1)} = -\frac{W}{K^2} (h_x S)^9. \quad (2.6)$$

For $V^{(2)}$, the transition can occur in several ways, six to be precise, corresponding to where the S_+^4 term acts. Two of the ways to make the transition are $-5 \rightarrow -1 \rightarrow 0 \rightarrow 1 \rightarrow 2 \rightarrow 3 \rightarrow 4$, and $-5 \rightarrow -4 \rightarrow 0 \rightarrow 1 \rightarrow 2 \rightarrow 3 \rightarrow 4$. The product of matrix elements in each case is

$$\left(-\frac{h_x S}{2}\right)^5 \lambda_2 \langle 4 | S_+^9 | -5 \rangle = -2^4 W \lambda_2 (h_x S)^5. \quad (2.7)$$

The energy denominators, however, depend on the transition path, and are listed in Table I. Adding together all the contributions, we get

$$\begin{aligned} V^{(2)} &= 2^4 W \frac{2}{K} \left(\frac{1}{8} + \frac{1}{20} + \frac{20}{112} \right) (h_x S)^4 \lambda_2 \\ &= \frac{2^4 \times 99}{140} \frac{W}{K} (h_x S)^5 \lambda_2. \end{aligned} \quad (2.8)$$

Lastly, for $V^{(3)}$, there are three transition paths: (i) $-5 \rightarrow -1 \rightarrow 3 \rightarrow 4$, (ii) $-5 \rightarrow -1 \rightarrow 0 \rightarrow 4$, (iii) $-5 \rightarrow -4 \rightarrow 0 \rightarrow 4$. The transition element product for all three is

$$-2^8 W (h_x S) \lambda_2^2, \quad (2.9)$$

and the energy denominator product is 20×8 , 20×20 , and 8×20 , respectively. Thus,

$$V^{(3)} = -\frac{2^8 \times 3}{200} W(h_x S) \lambda_2^2. \quad (2.10)$$

Adding together $V^{(1)}$, $V^{(2)}$, and $V^{(3)}$, we obtain the net $V_{4,-5}$ (restoring the level quantum numbers). The condition for a diabolic point is that this quantity should vanish. In addition to $h_x = 0$, this happens when

$$\xi^2 - \frac{99K}{140}\xi + \frac{3K^2}{200} = 0, \quad (2.11)$$

where

$$\xi = \frac{1}{\lambda_2} \left(\frac{h_x S}{2} \right)^4. \quad (2.12)$$

Solving Eq. (2.11), we obtain

$$h_x = \frac{2}{5} \left\{ \frac{99}{280} \pm \left[\left(\frac{99}{280} \right)^2 - \frac{3}{200} \right]^{\frac{1}{2}} \right\}^{\frac{1}{4}} (K \lambda_2)^{\frac{1}{4}}. \quad (2.13)$$

With the scaled value $\lambda_2 = 2.16 \times 10^{-4}$ for $S = 5$, this yields $h_x = 0.2643$, and 0.6252 . Direct numerical diagonalization yields $h_x = 0.2669$, and 0.638 .

Readers will undoubtedly have noted that apart from an overall factor of h_x to some power, our perturbation method yields the off-diagonal element as a homogeneous polynomial in h_x^4 and λ_2 . It is not difficult to see that this will be generally true, and also not difficult to justify. Let us first take the point that we have only included transition paths that go through the higher energy levels. Consider, e.g. the path for $V_{4,-5}$ in the above calculation that goes from -5 to $+1$ via six successive $h_x S_+$ terms, then to $+5$ via a CS_+^4 term, and finally to $+4$ via an $h_x S_-$ term. This term is of order $h_x^7 \lambda_2$, and should be regarded as a higher order correction to $V^{(2)}$. Secondly, it is positive and of the same sign as $V^{(2)}$, because it involves six negative and one positive energy denominator. This feature is also generally valid, and is important in light of the next point, which is that the sign of the terms in the polynomial for the off-diagonal element alternate when organized as a series in λ_2 . Thus, for $V_{4,-5}$, $V^{(1)}$ is negative, $V^{(2)}$ is positive, and $V^{(3)}$ is negative. This is a consequence of the fact that replacing four $-h_x S_+$ terms by a single CS_+^4 term (a) leaves the sign of the matrix element product unchanged, but (b) replaces four negative energy denominators by a single negative one.

Let us call the polynomial that remains after we have cancelled off as many overall factors of $h_x S$ from $V_{mm'}$ as possible the *underlying polynomial*. It is clear that this polynomial is of degree

$$n_{mm'} = \left\lfloor \frac{m - m'}{4} \right\rfloor, \quad (2.14)$$

in h_x^4 , where $[x]$ denotes the integer part of x , i.e., the largest integer less than or equal to x . The alternation of signs of successive powers of h_x^4 is a necessary (but not sufficient)

condition for all $n_{mm'}$ roots to be positive [19]. This means that, not including the points on the h_x or h_z axes, it is possible for states labelled by m and m' to intersect in a diabolical point *up to* $n_{mm'}$ times in the first quadrant of the h_x - h_z plane. This appears to us to be a topological property of the Mn_{12} Hamiltonian, that is not altered by presence of higher order terms, as long as the symmetry is not changed. Of course, the number of diabolical points may be fewer, but we do not believe it can be greater, because if h_x is sufficiently large, the term $H_x S_x$ dominates the energy in the equatorial plane, and the possibility of interfering trajectories is lost. We do not have a proof of these statements, which must be regarded as conjectures, but the similarity to Fe_8 , and all the empirical evidence we have gathered suggests that they are indeed true.

For $S = 5$, we have found all the diabolical points using this perturbation approach, and also numerically. In all cases, the perturbative answers are nearly exact. The results are shown in Fig. 2.

At this point we wish to note a remarkable feature of this approximation, which may have been noticed by some readers. This is that the diabolical values of h_x depend on m and m' only through the combination $\Delta m = m' - m$. This means that in Fig. 2, the theoretical points corresponding to the same value of $\Delta m = m' - m$ are vertically aligned. See, for example, the points corresponding to $m = -4, m' = 4$, and $m = -5, m' = 3$, or to $m = -5, m' = 2$, and $m = -4, m' = 3$. The reason is not hard to find. When we set $B = 0$, the energy E_m is a quadratic function of m , and when levels m and $m' > m$ are degenerate,

$$E_{m+k} - E_m = k(\Delta m - k). \quad (2.15)$$

Thus, *the entire pattern of energy levels above the levels m and m' depends only on Δm* (see Fig. 1), and since only these levels enter into our perturbation theory, the energy denominators are identical. The matrix elements are of course different, but since our transition paths involve no closed loops, they amount to a net factor of $\langle m' | S_+^{\Delta m} | m \rangle$ in each term, which therefore drops out of the underlying polynomial. In short, this polynomial depends only on Δm .

Furthermore, we see from Eq. (2.15) that value of S also does not enter in the energy denominators. This means that the polynomials found for $S = 5$ are applicable to the $S = 10$ problem for transitions with $\Delta m \leq 10$, and makes it worthwhile to find all the remaining polynomials for $S = 10$. The task is easily automated on a computer since the problem is essentially to enumerate the transition paths for a given order in h_x and λ_2 , and to add up the reciprocals of the corresponding energy denominators. It can be further simplified by noting that all denominators appear in the term proportional to $h_x^{\Delta m}$, so that relative to this term, the coefficient for any other transition path appears as an energy numerator, consisting of all the missing denominators. The polynomials are given in Table II, along with the roots for h_x for general S and λ_2 , as well as for the values applicable to Mn_{12} .

One last general point worth noting is that for a diabolical point labelled by the pair (m, m') with $m' > m$, the energy levels which are degenerate are numbers $2S + (m - m') + 1$ and $2S + (m - m') + 2$, where the ground state is given the number 1.

B. Inclusion of S_z^4 term

When we try and compare the results of the previous subsection with those obtained numerically from Eq. (1.1) with $B \neq 0$, we find that the systematics of the diabolical points are fully captured in that the analytic results provide a complete indexing scheme, but the quantitative disagreement with the Mn_{12} parameters is as bad as 30% in some cases. We therefore seek some way to incorporate the $B \neq 0$ effects.

It is easy to let $B \neq 0$ in the no-bias condition. Equation (2.3) is modified to

$$h_z(m, m') = -\frac{1}{S}(m + m') \left[1 + \lambda_1(m^2 + m'^2) \right]. \quad (2.16)$$

The no-mixing condition is clearly harder to evaluate. A simple minded approach is to shift the energy levels so as to retain the same relative spacings as when $B = 0$, but allow the overall range to be modified.

With this in mind, let us first consider the energies when $\lambda_1 = 0$. When levels m and m' are degenerate, the level at the top of the barrier is given by the quantum number $k = (m + m')/2$, whenever this is an integer, or by the nearest integers if it is a half-integer. In the spirit of our approximations, keeping track of this distinction would be an overrefinement, so we will use the formula $(m + m')/2$ in both cases. The energy range is thus given by

$$\Delta E^{(0)} = E_k^{(0)} - E_m^{(0)} = \frac{1}{4}(m - m')^2, \quad (2.17)$$

where the (0) superscript indicates that $B = 0$. With $B \neq 0$, we get

$$\begin{aligned} \Delta E^{(1)} &= \Delta E^{(0)} - \lambda_1 \left[\left(\frac{m + m'}{2} \right)^4 - m^4 \right] + \lambda_1(m + m')(m^2 + m'^2) \left[\frac{m + m'}{2} - m \right] \\ &= \gamma_{mm'} \Delta E^{(0)}, \end{aligned} \quad (2.18)$$

where

$$\gamma_{mm'} = 1 + \frac{\lambda_1}{4}(7m^2 + 10mm' + 7m'^2). \quad (2.19)$$

If we assume that the entire spectrum gets modified from its quadratic form by a uniform stretching factor $\gamma_{mm'}$, then the only change in our perturbation theory is that all energy denominators get multiplied by this factor. In the underlying polynomial, h_x and λ_2 get replaced by $h_x/\gamma_{mm'}$ and $\lambda_2/\gamma_{mm'}$, and hence the no-mixing condition becomes

$$h_x(m, m') = \gamma_{mm'}^{3/4} r_\alpha(\Delta m), \quad \alpha = 1, 2, \dots, n_{mm'}, \quad (2.20)$$

where $\{r_\alpha\}$ are the original h_x values obtained from the roots of the underlying polynomial $P_{\Delta m}$.

The formulas (2.16) and (2.20) are compared with exact numerical results in Table III. The errors are now typically about 10%, and can be of either sign.

It is useful to briefly discuss our numerical procedure. For points lying on the H_z or H_x axis, the splitting is a function of one variable, and its zeros can be found by simple scanning.

For the off-axis zeros, this is harder, and we resort to the Herzberg and Longuet-Higgins sign change theorem [14,20], which applied to the present problem states that, upon adiabatic traversal of a closed contour in the H_x - H_z plane enclosing a single point of degeneracy of two states, the wavefunction of either of these two states returns to itself except for a change in sign. Conversely, there is no change in sign if the contour does not enclose a degeneracy. Hence, to find a diabolical point, we first find a sign-reversing rectangular contour by hit and trial. By bisecting this rectangle in the x and z directions alternately, and using the sign-change test at each bisection, we can corral the degeneracy ever more tightly, to the degree desired. We have found this procedure to be generally superior to a direct minimization of the energy difference for the reason that the diabolical point in the vicinity of a degeneracy is highly asymmetrical in the x and z directions. Consider for example, the 4th and 5th energy levels from the bottom when $h_z \simeq 0.12$ – 0.13 , corresponding approximately to the m quantum numbers -9 and 8 . Since these states are separated by a high barrier, the mixing element between them is best understood as arising from tunneling, and will therefore be proportional to an exponentially small Gamow factor $e^{-\Gamma}$, where Γ is the appropriate tunneling action. Thus the energy surface consists of a deep and narrow valley running nearly parallel to the h_x axis, with a valley floor that goes to zero linearly at occasional points, and may rise and fall in between. Because of this shape, and because the surface is not analytic in the vicinity of the points being sought, standard methods for finding the minima of a function are often not well suited.

The above argument also enables to understand an observation made by Berry and Wilkinson [14] and Berry and Mondragon [21] in the study of two very different model problems, namely, that the energy cone near a diabolical point has very high eccentricity in terms of the physically natural parameters describing the system. In other words, the cross section of the energy surface is a very long and narrow ellipse in one direction. Let us see how this happens in the present problem. To save writing let us write just x and z for the deviations of h_x and h_z from a diabolical point at (h_{x0}, h_{z0}) . In the vicinity of this point, we have

$$B_{mm'} \simeq az, \quad (2.21)$$

$$V_{mm'} \simeq be^{-\Gamma}x, \quad (2.22)$$

where a and b are constants of order unity. Thus the energy surface is

$$E \simeq (a^2 z^2 + b^2 e^{-2\Gamma} x^2)^{1/2}. \quad (2.23)$$

The cross section is an ellipse with major axis parallel to x and eccentricity $\sim e^\Gamma \gg 1$. This scenario is expected to be quite general. The no-bias condition defines a line in parameter space. The gradient of the bias normal to this line is generally expected to be of order unity in the natural physical variables. The mixing element also varies on the same order unity scale in the parameter space, but because it arises from tunneling, its absolute scale is very small. The result is an energy surface of high eccentricity of the type just described.

C. Merged diabolical points [22]

Our discussion of diabolical points needs some elaboration for certain degeneracies lying on the h_z axis. For the pair $(m, m') = (-10, 9)$, e.g., (more generally any pair with $\Delta m =$

$4n + 3$), we peeled off a factor of h_x^3 from the mixing element. Writing $x = h_x$, and $z = h_z$ as in Eq. (2.23), and $z_0 = h_{z0}$ for the point of degeneracy, the bias and mixing are given by

$$B_{mm'} \approx z - z_0, \quad (2.24)$$

$$V_{mm'} \approx x^3 + O(x^7), \quad (2.25)$$

ignoring multiplicative constants. Correspondingly, the energy surface is $[(z - z_0)^2 + x^6]^{1/2}$, whose cross section is no longer an ellipse. There is also no reason for the simple sign-change result to hold a priori.

These conclusions are based on perturbation theory, however. More generally, we can only argue on grounds of symmetry that, under $x \rightarrow -x$, $B_{mm'} \rightarrow B_{mm'}$, and $V_{mm'} \rightarrow \pm V_{mm'}$. Instead of Eqs. (2.24) and (2.25), we should therefore expect the general expansion to take the form

$$B_{mm'} \approx z - z_0 + ax^2 + O((z - z_0)^2, x^2(z - z_0)^2, x^4), \quad (2.26)$$

$$V_{mm'} \approx x^3 - bx + cx(z - z_0) + O(x^3(z - z_0), x^5), \quad (2.27)$$

where a , b , and c are constants, all of which we expect to be very small on account of the quantitative accuracy of the perturbative approach. Ignoring the higher order terms, the bias vanishes on the parabola $z = z_0 - ax^2$. On this parabola, the mixing is given by

$$(1 - ac)x^3 - bx, \quad (2.28)$$

which vanishes at $x = 0$, and $x = \pm[b/(1 - ac)]^{1/2} \equiv \pm x_1$, assuming that $b/(1 - ac) > 0$. Thus instead of a single degeneracy at $(0, z_0)$, we have three closely spaced degeneracies at

$$(0, z_0), \quad (\pm x_1, z_0 - ax_1^2). \quad (2.29)$$

The energy surface in the immediate vicinity of each one of these points is now diabolical in the ordinary sense. A small circuit of each of these points separately will therefore lead to a sign reversal, as will a larger circuit enclosing all three of them. If we ignore the splitting, we may regard the original degeneracy on the h_z axis as a *triply merged* diabolical point.

It is useful to think of the coefficients a , b , and c as depending on parameters in the Hamiltonian other than the components of \mathbf{H} , e.g., λ_1 and λ_2 . It may be that as these parameters are varied, the quantity $b/(1 - ac)$ becomes negative, so that the roots $\pm x_1$ cease to be real. We can think of the two off-axis diabolical points as having annihilated each other, leaving behind only one true diabolical point on the axis. Unless one is very close to this point, however, the energy surface may still resemble that of a triply merged point.

For the parameters appropriate to Mn_{12} , we find that the points are located at [23]

$$(h_x, h_z) = (0.0, 0.135836224), \quad (\pm 0.01855, 0.135832551). \quad (2.30)$$

These numbers are obtained by using the same sign-reversal theorem as previously described. Because the energy difference depends so sensitively on h_z , however, we have confirmed them in another way. For any given value of h_x , we first find the minimum of the relevant energy gap Δ with respect to h_z . In essence, we find the value of the gap at the bottom of the parabolic trench where the bias vanishes. A plot of this gap versus h_x should be given by

the absolute value of the expression (2.28). As shown in Fig. 3, this is indeed so, and the split off point is again found to be at $h_x = 0.01855$.

In exactly the same way, we may also consider *doubly merged* points, corresponding to the tunneling of states with $\Delta m = 4n + 2$, e.g., $(m, m') = (-10, 8)$, when $h_x \approx 0$. We can continue to expand the bias as in Eq. (2.26), but the leading term in $V_{mm'}$ is now proportional to x^2 , so that instead of Eq. (2.27), we have

$$V_{mm'} \approx x^2 + O\left((z - z_0), x^2(z - z_0), x^4\right). \quad (2.31)$$

It is then obvious that the double zero of $V_{mm'}$ at $x = 0$ can not be split. This conclusion can also be reached in another way. Symmetry would require that, if they split, the points be located at $(\pm x_0, z_0)$, with $x_0 \neq 0$. The selection rule argument given at the very beginning of Sec. I shows, however, that this is impossible, as there must be a crossing of any two levels m and m' with $\Delta m \neq 4n$ as H_z is varied with $H_x = 0$. In Fig. 3, we also show the $(m, m') = (-10, 8)$ gap at the bottom of the no-bias trench. It is apparent that now the diabolical points remain unsplit at $h_x = 0$, and the curve is extremely well fit by a parabola, as required by Eq. (2.31).

Finally, the points on the h_z axis, corresponding to $\Delta m = 4n + 1$ are singly diabolical to begin with, so the issue of splitting does not arise.

III. SUMMARY

We have studied the diabolical points of a spin Hamiltonian describing molecules such as Mn_{12} that have an easy axis of four-fold symmetry, for arbitrarily directed magnetic fields. A perturbation theory in the parameters H_x and C is found to give a very good qualitative and even quantitative understanding. Our central results are the formulas (2.16) and (2.20), which along with the results in Table II give the full set of diabolical points for any molecule with $S \leq 10$.

ACKNOWLEDGMENTS

We are indebted to Wolfgang Wernsdorfer for very useful correspondence. AG's research is supported by the NSF via grant number DMR-9616749.

REFERENCES

- * Permanent address: Department of Physics, Dankook University, Cheonan, 330-714, Korea.
- ** Electronic address: agarg@northwestern.edu
- [1] See, e.g., the review by A. Caneschi et al., J. Magn. Magn. Mater. **200**, 182 (1999), and references therein.
- [2] M. A. Novak and R. Sessoli, in *Quantum Tunneling of Magnetization—QTM'94*, edited by L. Gunther and B. Barbara (Kluwer, Dordrecht, 1995).
- [3] J. Friedman, M. P. Sarachik, J. Tejada, and R. Ziolo, Phys. Rev. Lett. **76**, 3830 (1996).
- [4] L. Thomas et al., Nature **383**, 145 (1996).
- [5] C. Sangregorio, T. Ohm, C. Paulsen, R. Sessoli, and D. Gatteschi, Phys. Rev. Lett. **78**, 4645 (1997).
- [6] W. Wernsdorfer and R. Sessoli, Science **284**, 133 (1999).
- [7] D. Loss, D. P. DiVincenzo, and G. Grinstein, Phys. Rev. Lett. **69**, 3232 (1992); J. von Delft and C. L. Henley, *ibid* **69**, 3236 (1992).
- [8] A. Garg, Europhys. Lett. **22**, 205 (1993).
- [9] M. Wilkinson, Physica **21 D**, 341 (1986). See final paragraph of Sec. 6.
- [10] M. Stone, Kee-Su Park, and A. Garg, cond-mat/0004247 (to appear in J. Math. Phys.).
- [11] A.L. Barra, D. Gatteschi, and R. Sessoli, Phys. Rev. B **56**, 8192 (1997).
- [12] The spin coherent state $|\hat{\mathbf{n}}\rangle$, where $\hat{\mathbf{n}}$ is the direction with spherical polar coordinates (θ, ϕ) , is the state of maximum spin projection along $\hat{\mathbf{n}}$: $\mathbf{S} \cdot \hat{\mathbf{n}}|\hat{\mathbf{n}}\rangle = S|\hat{\mathbf{n}}\rangle$.
- [13] M. V. Berry and M. Wilkinson, Proc. Roy. Soc. Lond. A **392**, 15 (1984).
- [14] G. Herzberg and H. C. Longuet-Higgins, Discuss. Faraday Soc. **35**, 77 (1963).
- [15] A more rigorous argument is given in V. I. Arnold, *Mathematical Methods of Classical Mechanics* (Springer-Verlag, New York, 1978), Appendix 10.
- [16] J. Villain and A. Fort, Euro. Phys. J. B **17**, 69 (2000).
- [17] C.-S. Park and A. Garg, submitted to Phys. Rev. B. To avoid unnecessary repetition, we refer readers to this paper for a longer discussion of the setting of the problem, and references to background material, especially concerning the discrete phase integral method.
- [18] A. Garg, Europhys. Lett. **50**, 382, (2000).
- [19] Consider the polynomial $(x - a_1)(x - a_2) \cdots (x - a_n)$, where the a_i are all positive. The coefficient of x^{n-k} is $(-1)^k$ times the symmetric sum $\sum a_{i_1} a_{i_2} \cdots a_{i_k}$ of all distinct k -fold products of the a 's.
- [20] M. V. Berry, Proc. Roy. Soc. A **392**, 45 (1984).
- [21] M. V. Berry and R. J. Mondragon, J. Phys. A: Math. Gen. **19**, 873 (1986).
- [22] The considerations of this subsection were prompted by a private communication from Dr. Wernsdorfer, informing us that numerical diagonalization with the Mn₁₂ parameters revealed that in addition to being quenched on the h_z axis, the splitting of the $m = -10$ and $m' = 9$ states was also quenched at a very close by point.
- [23] Hence, $a = 1.067 \times 10^{-2}$. It seems safe to assume that $c \ll 1$, so that $b \simeq 3 \times 10^{-4}$.

FIGURES

FIG. 1. (a) Energy level diagram for $S = 5$, with $B = 0$, and $h_z = 1/5$. (b) Part of diagram for $S = 10$ with $h_z = 0.3$, showing that the pattern above any two degenerate levels depends only on Δm , irrespective of S .

FIG. 2. Diabolical points for $S = 5$. For λ_2 we have used the scaled value 2.16×10^{-4} . Each point is labeled by the Zeeman quantum numbers (m, m') except those on the h_z axis. Note that points with the same value of $m + m'$ are horizontally aligned, while those with the same $\Delta m = m' - m$ are vertically aligned. For the points on the h_z axis, any pair (m, m') is allowed, consistent with the given value of $m + m'$ and the rule $\Delta m \neq 4n$.

FIG. 3. Merged and nearly merged diabolical points. The plot shows the tunnel splitting $\Delta(m, m')$, showing how the triply merged $[(m, m') = (-10, 9)]$ point is split, but the doubly merged $[(m, m') = (-10, 8)]$ point is not. The splitting is calculated along the bottom of the parabolic trench in the h_x - h_z plane. In other words, for each value of h_x , what is plotted is the minimum of the splitting with respect to h_z . For the $-10 \leftrightarrow 9$ triple merger, also plotted is the curve $\Delta = |\alpha h_x (1 - h_x^2/h_{x1}^2)|$, with $\alpha = 1.51 \times 10^{-12}$, and $h_{x1} = 0.01855$, but this curve cannot be distinguished from the points on the scale of this figure, on account of the size and density of the symbols. (They can be distinguished on a large computer screen.) Similarly, the $-10 \leftrightarrow 8$ splitting is very accurately fit to a parabola.

TABLES

TABLE I. Transition paths and energy denominators for perturbative calculation of $V^{(2)}$.

Transition path	Energy denominator product
$-5 \rightarrow -1 \rightarrow 0 \rightarrow 1 \rightarrow 2 \rightarrow 3 \rightarrow 4$	$(-1)^5 20K$
$-5 \rightarrow -4 \rightarrow 0 \rightarrow 1 \rightarrow 2 \rightarrow 3 \rightarrow 4$	$(-1)^5 8K$
$-5 \rightarrow -4 \rightarrow -3 \rightarrow 1 \rightarrow 2 \rightarrow 3 \rightarrow 4$	$(-1)^5 (8 \times 14/20)K$
$-5 \rightarrow -4 \rightarrow -3 \rightarrow -2 \rightarrow 2 \rightarrow 3 \rightarrow 4$	$(-1)^5 (8 \times 14/20)K$
$-5 \rightarrow -4 \rightarrow -3 \rightarrow -2 \rightarrow -1 \rightarrow 3 \rightarrow 4$	$(-1)^5 8K$
$-5 \rightarrow -4 \rightarrow -3 \rightarrow -2 \rightarrow -1 \rightarrow 0 \rightarrow 4$	$(-1)^5 20K$

TABLE II. Underlying polynomials and h_x values for $S = 10$. In columns 1 and 2, $\Delta m = m' - m$ ($m' > m$), and $\xi = \lambda_2^{-1}(Sh_x/2)^4$. The quantity g is a convenient multiplier that enables reduction of the coefficients. Column 4 gives the fourth root of the roots of $P_{\Delta m}(\xi)$, i.e., the quantity $Sh_x/\lambda_2^{1/4}$. In column 5, we give the h_x values for $\lambda_2 = 5.4 \times 10^{-5}$ and $S = 10$.

Δm	$P_{\Delta m}(\xi)$	g	$Sh_x/\lambda_2^{1/4}$	h_x
4	$\xi - 36$	—	4.8990	0.04200
5	$\xi - 288$	—	8.2391	0.07063
6	$\xi - 1296$	—	12.000	0.1028
7	$\xi - 4320$	—	16.214	0.1390
8	$\xi^2 - 66g\xi + 49g^2$	180	6.8195, 20.821	0.05846, 0.1785
9	$\xi^2 - 99g\xi + 294g^2$	288	10.901, 25.785	0.09345, 0.2210
10	$\xi^2 - 429g\xi + 9604g^2$	144	15.286, 31.086	0.1310, 0.2665
11	$\xi^2 - 429g\xi + 13854g^2$	288	20.065, 36.703	0.1720, 0.3146
12	$\xi^3 - 1287g\xi^2 + 162171g^2\xi - 266805g^3$	180	8.3243, 25.185, 42.620	0.07136, 0.2159, 0.3654
13	$\xi^3 - 286g\xi^2 + 9767g^2\xi - 11858g^3$	1440	13.054, 30.620, 48.822	0.1119, 0.2625, 0.4185
14	$\xi^3 - 4862g\xi^2 + 3297473g^2\xi - 140612164g^3$	144	18.013, 36.357, 55.296	0.1544, 0.3116, 0.4740
15	$\xi^3 - 3978g\xi^2 + 2501703g^2\xi - 144597726g^3$	288	23.327, 42.383, 62.033	0.2000, 0.3633, 0.5318
16	$\xi^4 - 50388g\xi^3 + 444908598g^2\xi^2 - 474703246836g^3\xi + 6904413140625g^4$	36	9.600, 28.943, 48.684, 69.022	0.08230, 0.2481, 0.4173, 0.5917
17	$\xi^4 - 3876g\xi^3 + 2869532g^2\xi^2 - 315894768g^3\xi + 1301534080g^4$	720	14.907, 34.841, 55.251, 76.254	0.1278, 0.2987, 0.4736, 0.6537
18	$\xi^4 - 5814g\xi^3 + 6946761g^2\xi^2 - 1452656484g^3\xi + 20248151616g^4$	720	20.389, 41.013, 62.073, 83.721	0.1748, 0.3516, 0.5321, 0.7177
19	$\xi^4 - 21318g\xi^3 + 99462359g^2\xi^2 - 92627838402g^3\xi + 8455413407896g^4$	288	26.201, 47.448, 69.141, 91.417	0.2246, 0.4067, 0.5927, 0.7837
20	$\xi^5 - 245157g\xi^4 + 13893314634g^2\xi^3 - 175140030572298g^3\xi^2 + 285990169496161221g^4\xi - 648297466934390625g^5$	36	10.727, 32.285, 54.138, 76.448, 99.335	0.09196, 0.2768, 0.4641, 0.6553, 0.8515

TABLE III. Analytic and numerical results for diabolical point locations for the Mn_{12} Hamiltonian. For each pair (m, m') , the upper line lists the modified perturbation theory answers for (h_x, h_z) as given by Eqs. (2.20) and (2.16), and the lower line lists the numerical results. We have not separated the merged diabolical points located on the h_z axis (Sec. II C).

(m, m')	(h_x, h_z)				
$(-10, 10)$	(0.1053, 0.0)	(0.3169, 0.0)	(0.5314, 0.0)	(0.7504, 0.0)	(0.9751, 0.0)
	(0.1161, 0.0)	(0.3440, 0.0)	(0.5681, 0.0)	(0.7888, 0.0)	(1.0051, 0.0)
$(-9, 9)$	(0.0, 0.0)	(0.1954, 0.0)	(0.3931, 0.0)	(0.5949, 0.0)	(0.8024, 0.0)
	(0.0, 0.0)	(0.2097, 0.0)	(0.4161, 0.0)	(0.6206, 0.0)	(0.8234, 0.0)
$(-8, 8)$	(0.0900, 0.0)	(0.2713, 0.0)	(0.4564, 0.0)	(0.6471, 0.0)	
	(0.0953, 0.0)	(0.2836, 0.0)	(0.4711, 0.0)	(0.6587, 0.0)	
$(-7, 7)$	(0.0, 0.0)	(0.1655, 0.0)	(0.3341, 0.0)	(0.5081, 0.0)	
	(0.0, 0.0)	(0.1703, 0.0)	(0.3400, 0.0)	(0.5110, 0.0)	
$(-6, 6)$	(0.0751, 0.0)	(0.2273, 0.0)	(0.3847, 0.0)		
	(0.0759, 0.0)	(0.2273, 0.0)	(0.3803, 0.0)		
$(-5, 5)$	(0.1359, 0.0)	(0.2763, 0.0)			
	(0.1328, 0.0)	(0.2668, 0.0)			
$(-4, 4)$	(0.0598, 0.0)	(0.1827, 0.0)			
	(0.0569, 0.0)	(0.1708, 0.0)			
$(-3, 3)$	(0.1042, 0.0)				
	(0.0931, 0.0)				
$(-2, 2)$	(0.0422, 0.0)				
	(0.0353, 0.0)				
$(-1, 1)$	(0.0, 0.0)				
	(0.0, 0.0)				
$(-10, 9)$	(0.0, 0.1358)	(0.2546, 0.1358)	(0.4610, 0.1358)	(0.6717, 0.1358)	(0.8882, 0.1358)
	(0.0, 0.1358)	(0.2747, 0.1350)	(0.4904, 0.1332)	(0.7036, 0.1304)	(0.9139, 0.1263)
$(-9, 8)$	(0.0, 0.1287)	(0.1415, 0.1287)	(0.3308, 0.1287)	(0.5246, 0.1287)	(0.7240, 0.1287)
	(0.0, 0.1287)	(0.1507, 0.1284)	(0.3480, 0.1273)	(0.5445, 0.1252)	(0.7403, 0.1221)
$(-8, 7)$	(0.0, 0.1224)	(0.2169, 0.1224)	(0.3941, 0.1224)	(0.5767, 0.1224)	
	(0.0, 0.1224)	(0.2250, 0.1217)	(0.4040, 0.1204)	(0.5838, 0.1182)	
$(-7, 6)$	(0.0, 0.1168)	(0.1191, 0.1168)	(0.2794, 0.1168)	(0.4454, 0.1168)	
	(0.0, 0.1168)	(0.1215, 0.1166)	(0.2819, 0.1159)	(0.4444, 0.1146)	
$(-6, 5)$	(0.0, 0.1121)	(0.1801, 0.1121)	(0.3294, 0.1121)		
	(0.0, 0.1121)	(0.1781, 0.1118)	(0.3220, 0.1112)		
$(-5, 4)$	(0.0, 0.1081)	(0.0964, 0.1081)	(0.2281, 0.1081)		
	(0.0, 0.1081)	(0.0932, 0.1081)	(0.2170, 0.1081)		
$(-4, 3)$	(0.0, 1050)	(0.1418, 0.1050)			
	(0.0, 1049)	(0.1299, 0.1052)			

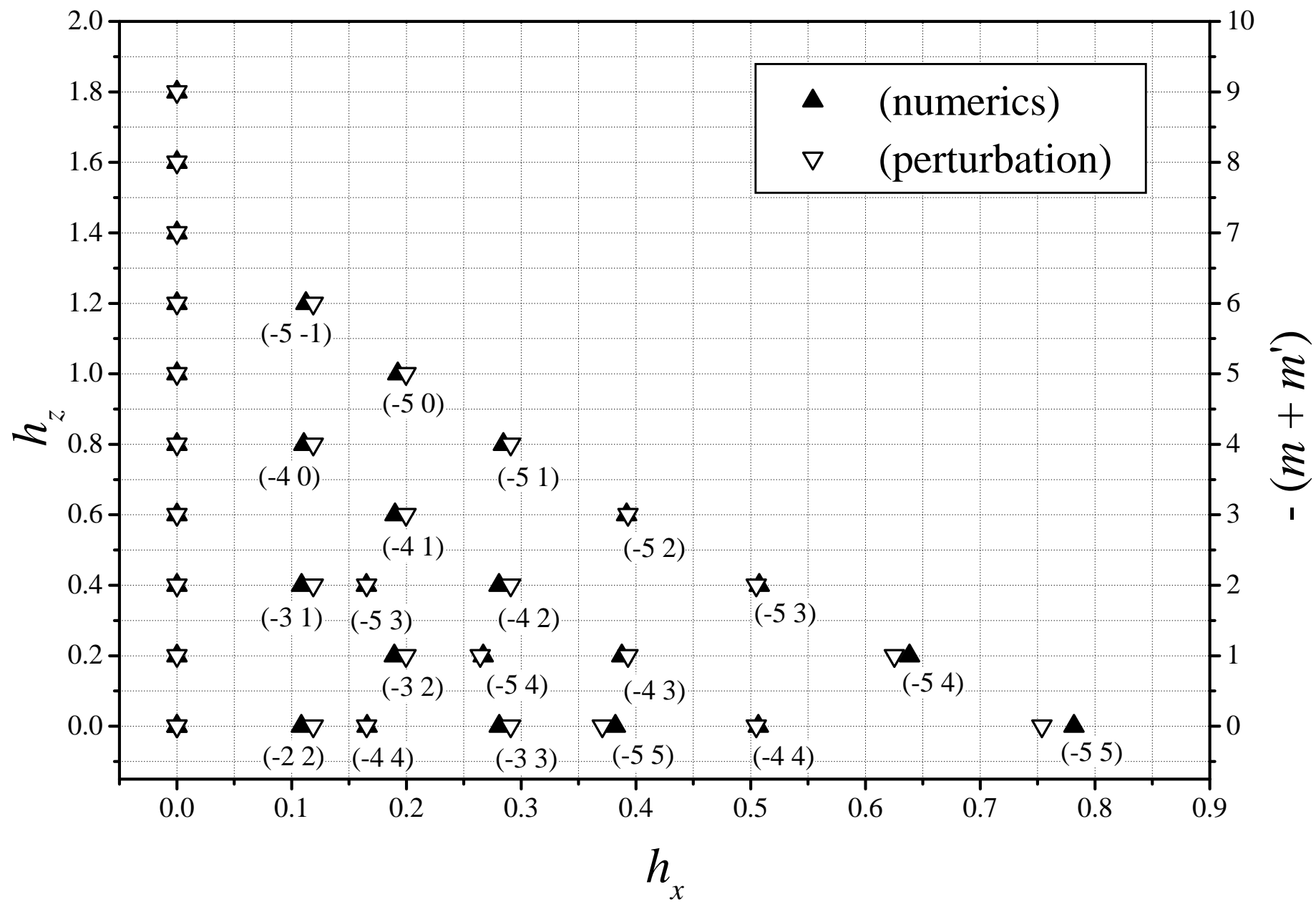
$(-3, 2)$	(0.0, 0.1026) (0.0, 0.1026)	(0.0714, 0.1026) (0.0625, 0.1028)			
$(-2, 1)$	(0.0, 0.1010) (0.0, 0.1009)				
$(-1, 0)$	(0.0, 0.1002) (0.0, 0.1001)				
$(-10, 8)$	(0.0, 0.2649) (0.0, 0.2649)	(0.1969, 0.2649) (0.2108, 0.2640)	(0.3961, 0.2649) (0.4186, 0.2610)	(0.5995, 0.2649) (0.6249, 0.2561)	(0.8085, 0.2649) (0.8298, 0.2491)
$(-9, 7)$	(0.0907, 0.2515) (0.0958, 0.2513)	(0.2735, 0.2515) (0.2854, 0.2495)	(0.4600, 0.2515) (0.4744, 0.2461)	(0.6522, 0.2515) (0.6638, 0.2409)	
$(-8, 6)$	(0.0, 0.2396) (0.0, 0.2396)	(0.1669, 0.2396) (0.1715, 0.2389)	(0.3368, 0.2396) (0.3425, 0.2368)	(0.5122, 0.2396) (0.5150, 0.2334)	
$(-7, 5)$	(0.0758, 0.2293) (0.0765, 0.2291)	(0.2292, 0.2293) (0.2290, 0.2282)	(0.3879, 0.2293) (0.3833, 0.2264)		
$(-6, 4)$	(0.0, 0.2206) (0.0, 0.2206)	(0.1370, 0.2206) (0.1339, 0.2203)	(0.2787, 0.2206) (0.2690, 0.2198)		
$(-5, 3)$	(0.0604, 0.2135) (0.0574, 0.2134)	(0.1843, 0.2135) (0.1724, 0.2138)			
$(-4, 2)$	(0.0, 0.2079) (0.0, 0.2079)	(0.1052, 0.2079) (0.0940, 0.2085)			
$(-3, 1)$	(0.0426, 0.2040) (0.0357, 0.2042)				
$(-2, 0)$	(0.0, 0.2016) (0.0, 0.2014)				
$(-10, 7)$	(0.0, 0.3885) (0.0, 0.3885)	(0.1437, 0.3885) (0.1525, 0.3877)	(0.3359, 0.3885) (0.3523, 0.3844)	(0.5327, 0.3885) (0.5520, 0.3782)	(0.7353, 0.3885) (0.7518, 0.3962)
$(-9, 6)$	(0.0, 0.3695) (0.0, 0.3695)	(0.2203, 0.3695) (0.2279, 0.3677)	(0.4003, 0.3695) (0.4097, 0.3637)	(0.5859, 0.3695) (0.5929, 0.3574)	
$(-8, 5)$	(0.0, 0.3529) (0.0, 0.3528)	(0.1210, 0.3529) (0.1232, 0.3523)	(0.2839, 0.3529) (0.2861, 0.3502)	(0.4527, 0.3529) (0.4514, 0.3464)	
$(-7, 4)$	(0.0, 0.3386) (0.0, 0.3385)	(0.1831, 0.3386) (0.1809, 0.3377)	(0.3349, 0.3386) (0.3273, 0.3361)		
$(-6, 3)$	(0.0, 0.3267) (0.0, 0.3267)	(0.0981, 0.3267) (0.0948, 0.3266)	(0.2320, 0.3267) (0.2209, 0.3266)		
$(-5, 2)$	(0.0, 0.3172) (0.0, 0.3171)	(0.1443, 0.3172) (0.1324, 0.3180)			
$(-4, 1)$	(0.0, 0.3101) (0.0, 0.3101)	(0.0727, 0.3101) (0.0637, 0.3108)			

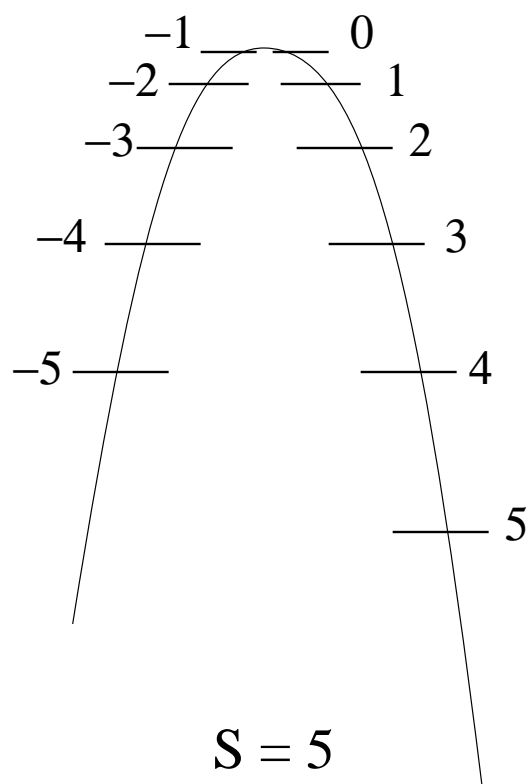
$(-3, 0)$	(0.0, 0.3053) (0.0, 0.3051)			
$(-2, -1)$	(0.0, 0.3030) (0.0, 0.3028)			
$(-10, 6)$	(0.0928, 0.5077) (0.0975, 0.5073)	(0.2799, 0.5077) (0.2909, 0.5040)	(0.4708, 0.5077) (0.4843, 0.4975)	(0.6674, 0.5077) (0.6791, 0.4876)
$(-9, 5)$	(0.0, 0.4840) (0.0, 0.4839)	(0.1709, 0.4840) (0.1750, 0.4826)	(0.3449, 0.4840) (0.3499, 0.4787)	(0.5245, 0.4840) (0.5270, 0.4722)
$(-8, 4)$	(0.0776, 0.4634) (0.0781, 0.4631)	(0.2349, 0.4634) (0.2342, 0.4613)	(0.3974, 0.4634) (0.3926, 0.4579)	
$(-7, 3)$	(0.0, 0.4459) (0.0, 0.4459)	(0.1405, 0.4459) (0.1372, 0.4454)	(0.2856, 0.4459) (0.2759, 0.4445)	
$(-6, 2)$	(0.0619, 0.4317) (0.0589, 0.4316)	(0.1890, 0.4317) (0.1771, 0.4323)		
$(-5, 1)$	(0.0, 0.4206) (0.0, 0.4205)	(0.1079, 0.4206) (0.0968, 0.4217)		
$(-4, 0)$	(0.0437, 0.4127) (0.0368, 0.4131)			
$(-3, -1)$	(0.0, 0.4079) (0.0, 0.4077)			
$(-10, 5)$	(0.0, 0.6238) (0.0, 0.6237)	(0.2272, 0.6237) (0.2338, 0.6209)	(0.4128, 0.6237) (0.4212, 0.6147)	(0.6042, 0.6237) (0.6110, 0.6049)
$(-9, 4)$	(0.0, 0.5960) (0.0, 0.5960)	(0.1249, 0.5960) (0.1266, 0.5952)	(0.2930, 0.5960) (0.2944, 0.5919)	(0.4672, 0.5960) (0.4656, 0.5861)
$(-8, 3)$	(0.0, 0.5723) (0.0, 0.5722)	(0.1890, 0.5723) (0.1865, 0.5709)	(0.3458, 0.5723) (0.3380, 0.5685)	
$(-7, 2)$	(0.0, 0.5525) (0.0, 0.5524)	(0.1014, 0.5525) (0.0979, 0.5523)	(0.2397, 0.5525) (0.2285, 0.5523)	
$(-6, 1)$	(0.0, 0.5366) (0.0, 0.5365)	(0.1491, 0.5366) (0.1373, 0.5379)		
$(-5, 0)$	(0.0, 0.5248) (0.0, 0.5247)	(0.0752, 0.5248) (0.0663, 0.5258)		
$(-4, -1)$	(0.0, 0.5168) (0.0, 0.5165)			
$(-3, -2)$	(0.0, 0.5129) (0.0, 0.5126)			
$(-10, 4)$	(0.0, 0.7378) (0.0, 0.7377)	(0.1775, 0.7378) (0.1808, 0.7359)	(0.3582, 0.7378) (0.3622, 0.7306)	(0.5448, 0.7378) (0.5470, 0.7217)

(-9, 3)	(0.0807, 0.7069)	(0.2441, 0.7069)	(0.4132, 0.7069)	
	(0.0809, 0.7065)	(0.2429, 0.7041)	(0.4080, 0.6995)	
(-8, 2)	(0.0, 0.6808)	(0.1461, 0.6808)	(0.2972, 0.6808)	
	(0.0, 0.6807)	(0.1426, 0.6802)	(0.2873, 0.6790)	
(-7, 1)	(0.0644, 0.6594)	(0.1967, 0.6594)		
	(0.0614, 0.6594)	(0.1849, 0.6604)		
(-6, 0)	(0.0, 0.6428)	(0.1123, 0.6428)		
	(0.0, 0.6427)	(0.1015, 0.6443)		
(-5, -1)	(0.0456, 0.6309)			
	(0.0387, 0.6316)			
(-4, -2)	(0.0, 0.6238)			
	(0.0, 0.6235)			
(-10, 3)	(0.0, 0.8511)	(0.1306, 0.8511)	(0.3064, 0.8511)	(0.4886, 0.8511)
	(0.0, 0.8510)	(0.1317, 0.8501)	(0.3070, 0.8459)	(0.4867, 0.8385)
(-9, 2)	(0.0, 0.8178)	(0.1979, 0.8178)	(0.3620, 0.8178)	
	(0.0, 0.8177)	(0.1949, 0.8162)	(0.3451, 0.8131)	
(-8, 1)	(0.0, 0.7901)	(0.1062, 0.7901)	(0.2511, 0.7901)	
	(0.0, 0.7900)	(0.1026, 0.7899)	(0.2400, 0.7901)	
(-7, 0)	(0.0, 0.7679)	(0.1563, 0.7679)		
	(0.0, 0.7678)	(0.1448, 0.7697)		
(-6, -1)	(0.0, 0.7513)	(0.0788, 0.7513)		
	(0.0, 0.7512)	(0.0701, 0.7528)		
(-5, -2)	(0.0, 0.7402)			
	(0.0, 0.7399)			
(-4, -3)	(0.0, 0.7347)			
	(0.0, 0.7344)			
(-10, 2)	(0.0849, 0.9647)	(0.2570, 0.9647)	(0.4348, 0.9647)	
	(0.0848, 0.9643)	(0.2551, 0.9614)	(0.4296, 0.9559)	
(-9, 1)	(0.0, 0.9299)	(0.1539, 0.9299)	(0.3131, 0.9299)	
	(0.0, 0.9298)	(0.1501, 0.9292)	(0.3032, 0.9278)	
(-8, 0)	(0.0679, 0.9014)	(0.2074, 0.9014)		
	(0.0648, 0.9014)	(0.1959, 0.9027)		
(-7, -1)	(0.0, 0.8792)	(0.1185, 0.8792)		
	(0.0, 0.8791)	(0.1080, 0.8812)		
(-6, -2)	(0.0481, 0.8634)			
	(0.0414, 0.8643)			
(-5, -3)	(0.0, 0.8539)			

	(0.0, 0.8536)		
(-10, 1)	(0.0, 1.0800) (0.0, 1.0799)	(0.2095, 1.0800) (0.2061, 1.0782)	(0.3832, 1.0800) (0.3753, 1.0747)
(-9, 0)	(0.0, 1.0443) (0.0, 1.0443)	(0.1125, 1.0443) (0.1089, 1.0442)	(0.2661, 1.0443) (0.2553, 1.0444)
(-8, -1)	(0.0, 1.0158) (0.0, 1.0158)	(0.1658, 1.0158) (0.1547, 1.0179)	
(-7, -2)	(0.0, 0.9944) (0.0, 0.9944)	(0.0836, 0.9944) (0.0753, 0.9962)	
(-6, -3)	(0.0, 0.9802) (0.0, 0.9799)		
(-5, -4)	(0.0, 0.9731) (0.0, 0.9729)		
(-10, 0)	(0.0, 1.1980) (0.0, 1.1979)	(0.1638, 1.1980) (0.1599, 1.1973)	(0.3331, 1.1980) (0.3237, 1.1957)
(-9, -1)	(0.0723, 1.1624) (0.0693, 1.1624)	(0.2209, 1.1624) (0.2099, 1.1638)	
(-8, -2)	(0.0, 1.1346) (0.0, 1.1346)	(0.1263, 1.1346) (0.1164, 1.1369)	
(-7, -3)	(0.0513, 1.1148) (0.0449, 1.1160)		
(-6, -4)	(0.0, 1.1030) (0.0, 1.1028)		
(-10, -1)	(0.0, 1.3200) (0.0, 1.3199)	(0.1202, 1.3200) (0.1167, 1.3199)	(0.2844, 1.3200) (0.2743, 1.3200)
(-9, -2)	(0.0, 1.2851) (0.0, 1.2851)	(0.1773, 1.2851) (0.1670, 1.2873)	
(-8, -3)	(0.0, 1.2590) (0.0, 1.2590)	(0.0895, 1.2590) (0.0817, 1.2609)	
(-7, -4)	(0.0, 1.2416) (0.0, 1.2414)		
(-6, -5)	(0.0, 1.2329) (0.0, 1.2328)		
(-10, -2)	(0.0776, 1.4471) (0.0748, 1.4472)	(0.2370, 1.4471) (0.2271, 1.4485)	
(-9, -3)	(0.0, 1.4138) (0.0, 1.4138)	(0.1356, 1.4138) (0.1266, 1.4161)	
(-8, -4)	(0.0551, 1.3901)		

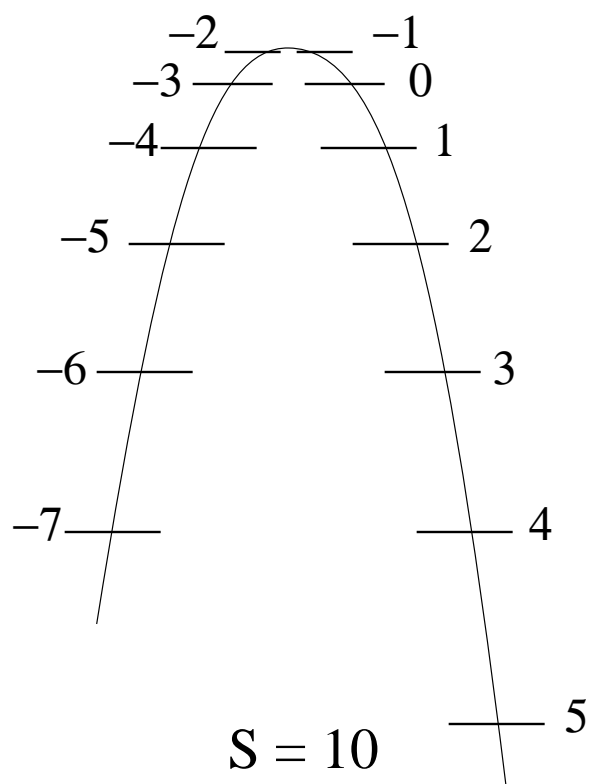
	(0.0492, 1.3913)	
$(-7, -5)$	(0.0, 1.3758)	
	(0.0, 1.3758)	
$(-10, -3)$	(0.0, 1.5806)	(0.1909, 1.5806)
	(0.0, 1.5806)	(0.1818, 1.5826)
$(-9, -4)$	(0.0, 1.5497)	(0.0964, 1.5497)
	(0.0, 1.5497)	(0.0895, 1.5516)
$(-8, -5)$	(0.0, 1.5291)	
	(0.0, 1.5291)	
$(-7, -6)$	(0.0, 1.5188)	
	(0.0, 1.5188)	
$(-10, -4)$	(0.0, 1.7216)	(0.1463, 1.7216)
	(0.0, 1.7216)	(0.1387, 1.7236)
$(-9, -5)$	(0.0595, 1.6938)	
	(0.0544, 1.6950)	
$(-8, -6)$	(0.0, 1.6772)	
	(0.0, 1.6772)	
$(-10, -5)$	(0.0, 1.8713)	(0.1043, 1.8713)
	(0.0, 1.8713)	(0.0985, 1.8729)
$(-9, -6)$	(0.0, 1.8475)	
	(0.0, 1.8475)	
$(-8, -7)$	(0.0, 1.8356)	
	(0.0, 1.8357)	
$(-10, -6)$	(0.0644, 2.0308)	
	(0.0604, 2.0318)	
$(-9, -7)$	(0.0, 2.0118)	
	(0.0, 2.0119)	
$(-10, -7)$	(0.0, 2.2015)	
	(0.0, 2.2016)	
$(-9, -8)$	(0.0, 2.1881)	
	(0.0, 2.1881)	
$(-10, -8)$	(0.0, 2.3845)	
	(0.0, 2.3846)	
$(-10, -9)$	(0.0, 2.5809)	
	(0.0, 2.5810)	





$$S = 5$$

(a)



$$S = 10$$

(b)

